2

Application of Bio-Inspired Algorithms and Neural Networks for Optimal Design of Fractal Frequency Selective Surfaces

Paulo Henrique da Fonseca Silva[1], Marcelo Ribeiro da Silva[2], Clarissa de Lucena Nóbrega[2] and Adaildo Gomes D'Assunção[2]
[1]*Federal Institute of Education, Science and Technology of Paraiba, IFPB,*
[2]*Federal University of Rio Grande do Norte, UFRN,*
Brazil

1. Introduction

Technological advances in the field of microwave and communication systems and the increase of their commercial applications in recent years have resulted in more stringent requirements for innovative design of microwave passive devices, such as: antennas, filters, power splitters and couplers, frequency selective surfaces, etc. To be competitive in the commercial marketplace, microwave engineers may be using computer-aided design (CAD) tools to minimize cost and design cycle times. Modern CAD tools have become an integral part of the microwave product cycle and demand powerful optimization techniques combined with fast and accurate models so that the optimal solutions can be achieved, eventually guaranteeing first-pass design success. The target of microwave device design is to determine a set of physical parameters to satisfy certain design specifications (Mohamed, 2005).

Early methods of designing and optimizing microwave devices by hand are time and labor intensive, limit complexity, and require significant expertise and experience. Many of the important developments in microwave engineering were made possible when complex electromagnetic characteristics of microwave devices were represented in terms of circuit equivalents, lumped elements and transmission lines. Circuit simulators using empirical/analytical models are simple and efficient, reduce optimization time, but have limited accuracy or validity region. Although circuit simulator is still used today it suffers from some severe limitations (the most serious of them is that it considers only fundamental mode interactions) and requires corrections in the form of post manufacturing tuning (Fahmi, 2007).

While developments in circuit simulators were taking place, numerical electromagnetic (EM) techniques were also emerging. With the computational power provided by modern computers, the use of accurate full-wave electromagnetic models by EM simulators for design and optimization of microwave devices became possible. By using full-wave electromagnetic methods higher order modes are taken into consideration and microwave devices can be rigorously characterized in the designs so that simulation and experimental results are in close agreement. This is particularly of interest for the rapid large scale

production of low-cost high performance microwave devices reducing or eliminating the need of post manufacturing tuning (Bandler et al., 1994; Fahmi, 2007).

The EM simulators can simulate microwave device structures of arbitrary geometrical shapes and ensure a satisfactory degree of accuracy up to millimeter wave frequencies (Mohamed, 2005). These simulators are based on EM field solvers whose function is to solve the EM problem of the structure under analysis, which is described by the Maxwell´s equations. Thus, the design of electromagnetic structures is usually a very challenging task due to the complexity of the models involved. In the majority of cases, there are no simple analytical formulas to describe the performance of new microwave devices. However, the use of EM field solver for device optimization is still a time consuming procedure and need heavy computations. For complex problems, resulting in very long design cycles, this computational cost may be prohibitive (Haupt & Werner, 2007).

Actually, many approaches are available to implement optimization using full-wave methods. For instance, the exploitation of commercial EM software packages inside the optimization loop of a general purpose optimization program. New techniques, such as geometry capture (Bandler et al., 1996) (suitable for automated EM design of arbitrary three-dimensional structures), space mapping (Bandler et al., 1994) (alternative design schemes combining the speed of circuit simulators with the accuracy of EM solvers), adjoint network concept (Nikolova et al., 2004), global optimization techniques based on bio-inspired algorithms, knowledge based methods, and artificial neural networks (ANNs), establish a solid foundation for efficient optimization of microwave device structures (Haupt & Werner, 2007; Zhang & Gupta, 2000; Silva et al., 2010a).

This chapter presents a new fast and accurate EM optimization technique combining full-wave method of moments (MoM), bio-inspired algorithms, continuous genetic algorithm (GA) and particle swarm optimization (PSO), and multilayer perceptrons (MLP) artificial neural networks. The proposed optimization technique is applied for optimal design of frequency selective surfaces with fractal patch elements. A fixed FSS screen geometry is choose a priori and then optimizing a smaller subset of FSS design variables to achieve a desired bandstop filter specification.

A frequency selective surface (FSS) is a two-dimensional array of periodic metallic elements on a dielectric layer or two-dimensional arrays of apertures within a metallic screen. This surface exhibits total reflection or transmission for patch and aperture elements, respectively. The most important parameters that will determine the overall frequency response of a FSS are: element shape, cell size, orientation, and dielectric layer properties. FSSs have been widely used as spatial filters for plane waves in a variety of applications, such as: microwave, optical, and infrared filters, bandpass radomes, microwave absorbers, polarizers, dichroic subreflectors, antenna systems, etc. (Munk, 2000).

Several authors proposed the design of FSS using fractals. In this chapter, different fractal geometries are considered, such as: Koch, Dürer's pentagon, and Sierpinski. While the use of space-filling fractal properties (e.g., Koch, Minkowski, Hilbert) reduce the overall size of the FSS elements (Oliveira et al., 2009; Campos et al., 2010), the attractive features of certain self-similar fractals (e.g., Sierpinski, Gosper, fractal tree, etc.) have received attention of microwave engineers to design multiband FSS. Many others self-similar geometries have been explored in the design of dual-band and dual polarized FSS (Gianvittorio et al., 2001).

The self-similarity property of these fractals enables the design of multiband fractal elements or fractal screens (Gianvittorio et al., 2003). Furthermore, as the number of fractal iterations increases, the resonant frequencies of these periodic structures decrease, allowing the construction of compact FSSs (Cruz et al., 2009). In addition, an FSS with fractal elements present resonant frequency that is almost independent of the plane-wave incidence angle.

There is no closed form solution directly from a given desired frequency response to the corresponding FSS with fractal elements. The analysis of scattering characteristics from FSS devices requires the application of rigorous full-wave techniques. Besides that, due to the computational complexity of using a full-wave simulator to evaluate the FSS scattering variables, many electromagnetic engineers still use trial-and-error process until to achieve a given design criteria. Obviously this procedure is very laborious and human dependent. On the other hand, calculating the gradient of the scattering coefficients in terms of the FSS design variables is quite difficult. Therefore, optimization techniques are required to design practical FSSs with desired filter specifications. Some authors have been employed neural networks, PSO, and GA for FSS design and optimization (Manara et al., 1999; Hussein & El-Ghazaly, 2004; Silva et al., 2010b).

The main computational drawback for EM optimization of FSSs based on bio-inspired algorithms relies on the repetitive evaluation of numerically expensive fitness functions. Due the expensive computation to calculate the scattering variables for every population member at multiple frequencies over many generations, several schemes are available to improve the GA performance for optimal design of FSSs, such as: the use of fast full-wave methods, micro-genetic algorithm, which aims to reduce the population size, and parallel GA using parallel computation. However, despite of these improvements done on the EM optimization using genetic algorithms, all the same several hours are required for expensive computational simulations of GA optimization (Haupt & Werner, 2007; Silva et al., 2010b).

The application of ANNs as approximate fitness evaluation tools for genetic algorithms, though suggest often, had seldom been put to practice. The combination of ANNs and GAs has been applied mainly for the construction of optimized neural networks through GA-based optimization techniques. Few applications of ANNs to GA processing have been reported for EM optimization of microwave devices.

The advantages of the MoM-ANN-GA/PSO optimization technique are discussed in terms of convergence and computational cost. This technique is applied for optimal design of bandstop FSS spatial filters with fractal elements considering the resonant frequency (*fr*) and bandwidth (*BW*) bandstop specifications. Some FSS prototypes with fractal elements are built and measured. The accuracy of the proposed optimization technique is verified by means of comparisons between theoretical and experimental results.

2. An overview of bio-inspired optimization technique

The idea of blending full-wave methods, artificial neural networks, and bio-inspired optimization algorithms for electromagnetic optimization of FSS spatial filters was first proposed in 2007 (Silva et al., 2007). This optimization technique named MoM-ANN-GA replaces the computational intensive full-wave method of moments simulations by a fast and accurate MLP neural network model of FSS spatial filter, which is used to compute the cost (or fitness) function in the genetic algorithm iterations.

The proposed bio-inspired EM optimization technique starts with the definition of a FSS screen geometry that is choose a priori. A full-wave parametric analysis is carried out for accurate EM characterization of FSS spatial filter scattering properties. From obtained EM dataset, a MLP network is trained to establish the complicated relationships between FSS design variables and frequency response. Then, in order to overcome the computational requirements associated with full-wave numerical simulations, the developed MLP model is used for fast and accurate evaluation of fitness function into bio-inspired algorithm simulations. From the optimal design of FSS parameters, FSS prototypes are fabricated and measured for verification of optimization methodology. Fig. 1 gives a "big picture" overview of proposed bio-inspired EM optimization technique.

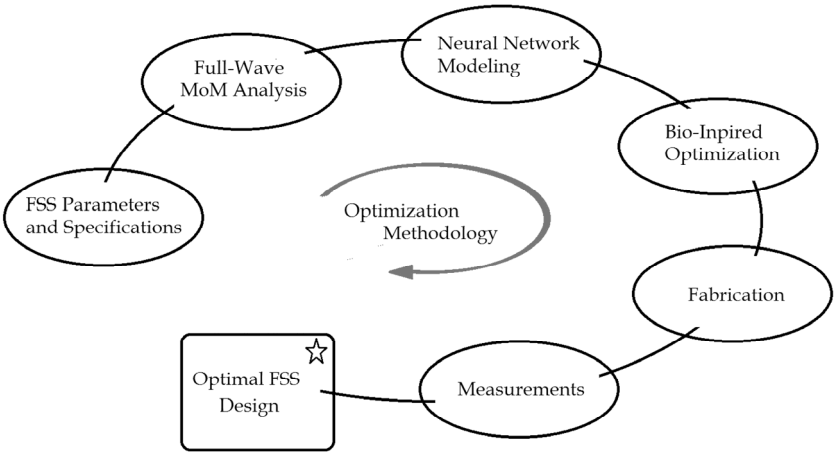

Fig. 1. An overview of proposed bio-inspired optimization technique

This section is a brief introduction that provides an overview of the proposed optimization technique to be presented. The overview includes fundamentals of multilayer perceptrons, continuous genetic algorithm, and particle swarm optimization.

2.1 Artificial neural networks

Since the beginning of the 1990s, the artificial neural networks have been used as a flexible numerical tool, which are efficient for modeling of microwave devices. In the CAD applications related to microwave engineering, the use of ANNs as nonlinear models becomes very common. Neural network models trained by accurate EM data (obtained through measurements or by EM simulations) are used for fast and accurate design/optimization of microwave devices. In addition, the use of previously established knowledge in the microwave area (as empirical models) combined with the neural networks, results in a major reliability of the resulting hybrid model – with a major ability to learn nonlinear input-output mappings, as well as to generalize responses, when new values of the input design variables are presented. Another important advantage is the data amount reduction necessary for the neural networks training. Some hybrid modeling techniques have been proposed for the use with empirical models and neural networks, such as: Source Difference Method, PKI (Prior Knowledge Input), KBNN (Knowledge Based

Neural Network), and SMANN (Space Mapping Artificial Neural Network) (Zhang & Gupta, 2000).

Versatility, efficient computation, reduced memory occupation, stability of learning algorithms, and generalization from representative data, are some characteristics that have motivated the use of neural networks in many areas of microwave engineering as models for complex ill-defined input-output mappings in new, not well-known microwave devices (Santos et al., 1997; Patnaik & Mishra, 2000; Zhang & Gupta, 2000). As mentioned previously, the electromagnetic behavior of a microwave device is extremely complex and simple empirical model cannot accurately describe its behavior under all conditions. Only with a detailed full-wave device model, more accurate results can be found. In general, the quality of simulation is decided by the accuracy of device models. On the other hand, a very detailed model would naturally slow down the program. A compromise between accuracy and speed of computation has to be struck. Using neural networks enables to overcome this problem (Silva et al., 2010a).

The multilayer perceptrons is the most used artificial neural network for neuromodeling applications. Multilayer perceptrons artificial neurons are based on the nonlinear model proposed by (McCulloch & Pitts, 1943; Rosenblatt, 1958, as cited in Haykin, 1999). In this model, neurons are signal processing units composed by a linear combiner and an activation function, that can be linear or nonlinear, as shown in Fig. 2.

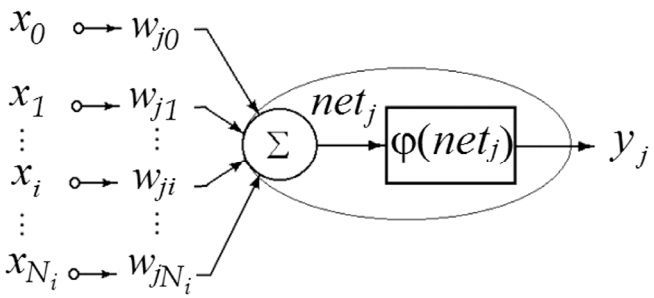

Fig. 2. Nonlinear model of an artificial neuron

The input signals are defined as x_i, $i = 0,1,\cdots,N_i$, where N_i is the number of input units. The output of linear combiner corresponds to the neuron level of internal activity net_j, as defined in (1). The information processed by neuron is storage in weights w_{ji}, $j = 1,\cdots,N_j$, where N_j is the number of neurons in a given neural network layer; $x_0 = \pm 1$ is the polarization potential (or threshold) applied to the neurons. The neuron output signal y_j is the value of the activation function $\varphi(\cdot)$ in response to the neuron activation potential net_j, as defined in (2).

$$net_j = \sum_{i=0}^{Ni} w_{ji} \cdot x_i \tag{1}$$

$$y_j = \varphi(net_j) \tag{2}$$

Multilayer perceptrons presents a feed forward neural network (FNN) configuration with neurons set into layers. Each neuron of a layer is connected to those of the previous layer, as illustrated in Fig. 3. Signal propagation occurs from input to output layers, passing through the hidden layers of the FNN. Hidden neurons represent the input characteristics, while output neurons generate the neural network responses (Haykin, 1999).

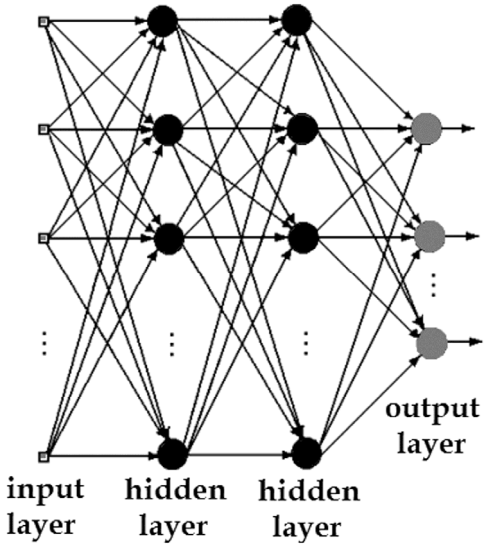

Fig. 3. Feed forward neural network configuration with two hidden layers

The design of a MLP model consists by three main steps: i) configuration – how layers are organized and connected; ii) supervised learning – how information is stored in neural network; iii) generalization test – how neural network produces reasonable outputs for inputs not found in the training set (Haykin, 1999). In this work, we use feed forward neural networks and supervised learning to develop MLP neural network models.

In the computational simulation of supervised error-correcting learning, a training algorithm is used for the adaptation of neural network synaptic weights. The instantaneous error $\mathbf{e}(\mathrm{n})$, as defined in (3), represents the difference between the desired response $\mathbf{d}(\mathrm{n})$, and the neural network output $\mathbf{y}(n)$, at the n-th iteration, corresponding to the presentation of the n-th training example, $(\mathbf{x}(\mathrm{n});\mathbf{d}(\mathrm{n}))$. Training examples variables are normalized to present unitary maximum absolute value. So, when using a given MLP model, prior scaling and de-scaling operations may be performed into input and output signals of MLP neural network, according to (4) and (5), respectively.

$$\mathbf{e}(n) = \mathbf{y}(n) - \mathbf{d}(n) \tag{3}$$

$$\overline{\mathbf{x}} = \mathbf{x} / \mathbf{x}_{\max} \tag{4}$$

$$\mathbf{y} = \overline{\mathbf{y}} \cdot \mathbf{y}_{\max} \tag{5}$$

Supervised learning has as objective the minimization of the sum squared error SSE(t), given in (6), where the index t, represents the number of training epochs (one complete presentation of all training examples, $n = 1, 2, \ldots, N$, where N is the total number of examples, is called an epoch).

$$SSE(t) = \frac{1}{N \cdot N_j} \sum_{n=1}^{N} \sum_{j=1}^{Nj} \frac{1}{2} e_j(n)^2 \tag{6}$$

Currently, there are several algorithms for the training of MLP neural networks. The most popular training algorithms are those derived from back-propagation algorithm (Rumelhart, Hinton, & Williams, 1986, as cited in Haykin, 1999). Among the family of back-propagation algorithms, the RPROP algorithm shows to be very efficient in solving complex modeling learning tasks.

After neural network training, we hope that MLP weights will storage the representative information contained on training dataset. The trained neural network is tested in order to verify its capability of generalizing to new values that do not belong to the training dataset. Therefore, the MLP neural network operates like a "black box" model inside a given region of interest, which was previously defined when the training dataset was generated.

2.2 Bio-inspired optimization algorithms

Bio-inspired algorithms, which are stochastic population-based global search methods inspired by nature, such as simulated annealing (SA), genetic algorithm and particle swarm optimization are effective for optimization problems with a large number of design variables and inexpensive fitness function evaluation (Haupt, 1995; Haupt & Werner, 2007; Kennedy & Eberhart, 1995). However, the main computational drawback for optimization of microwave devices relies on the repetitive evaluation of numerically expensive fitness functions. Finding a way to shorten the optimization cycle is highly desirable (Silva et al., 2010b). For instance, several GA schemes are available in order to improve its performance, such as: the use of fast full-wave methods, micro-genetic algorithm, which aims to reduce the population size, and parallel GA using parallel computation (R. L. Haupt & Sue, 2004).

Bio-inspired algorithms start with an initial population of candidate individuals for the optimal solution. Assuming an optimization problem with N_{var} input variables and N_{pop} individuals, the population at the i-th iteration is represented as a matrix $\boldsymbol{P}(i)_{Npop \times Nvar}$ of floating-point elements, denoted by $p^i_{m,n}$, with each row corresponding to an individual. Under GA and PSO jargons, the individuals are named *chromosomes* and *particles* (or agents), respectively.

2.2.1 Continuous genetic algorithm

Continuous genetic algorithm is very similar to the binary-GA but works with floating-point variables. Continuous-GA chromosomes are defined in (7) as a vector with N_{var} floating-point optimization variables. Each chromosome is evaluated by means of its associated cost, which is computed through the cost function E given in (8).

$$chromosome(\mathrm{i},m) = \left[p^{i}_{m,1}, \quad p^{i}_{m,2}, \quad \ldots, \quad p^{i}_{m,N\,\mathrm{var}} \right], \quad m = 1,2,\ldots,Npop \tag{7}$$

$$\cos t(\mathrm{i},m) = \mathbf{E}\left(chromosome(\mathrm{i},m)\right) \tag{8}$$

Based on the cost associated to each chromosome, the population evolves through generations with the application of genetic operators, such as: selection, crossover and mutation. Flow chart shown in Fig. 4(a) gives an overview of continuous-GA.

Mating step includes roulette wheel selection presented in (Haupt & Werner, 2007; R. L. Haupt & Sue, 2004). Population selection is performed after the N_{pop} chromosomes are ranked from lowest to highest costs. Then, the N_{keep} most-fit chromosomes are selected to form the mating pool and the rest are discarded to make room for the new offspring. Mothers and fathers pair in a random fashion through the blending crossover method (R. L. Haupt & Sue, 2004). Each pair produces two offspring that contain traits from each parent. In addition, the parents survive to be part of the next generation. After mating, a fraction of chromosomes in the population will suffer mutation. Then, the chromosome variable selected for real-value mutation is added to a normally distributed random number.

Most users of continuous-GA add a normally distributed random number to the variable selected for mutation with a constant standard deviation (R. L. Haupt & Sue, 2004). In particular, we propose a new real-value mutation operator for continuous-GA as given in (9), where p_{max} and p_{min} are constant values defined according to the limits of the region of interest composed by input parameters. Function *randn*() returns a normal distribution with mean equal to zero and standard deviation equal to one.

This mutation operator was inspired by simulating annealing cooling schedules (R. L. Haupt & Sue, 2004). It is used to improve continuous-GA convergence at the neighbourhood of global minimum. The quotient function Q given in (10) is crescent when the number of iterations increases and the global cost decreases. Thus, similar to the decrease of temperature in a simulating annealing algorithm, the standard deviation is decreased when the number of continuous-GA iterations is increased. The parameter A is a constant value and B is a value of cost function neighbour to the global minimum. The continuous-GA using the real-value mutation definition given in (9) and (10) is denominated improved genetic algorithm.

$$p^{i+1}_{m,n} = p^{i}_{m,n} + randn() \cdot \frac{\left(p_{\max} - p_{\min}\right)}{Q\left(i, global\cos t(i)\right)} \tag{9}$$

$$Q\left(i, global\cos t(i)\right) = \begin{cases} A, & global\cos t(i) \geq B \\ A + i \cdot \left[\log\left(global\cos t(i)\right)\right]^{2}, & global\cos t(i) < B \end{cases} \tag{10}$$

2.2.2 Particle swarm optimization

Particle swarm optimization was first formulated in 1995 (Kennedy & Eberhart, 1995). The thought process behind the algorithm was inspired by social behavior of animals, such as bird flocking or fish schooling. PSO is similar to continuous-GA since it begins with a

random initial population. Unlike GA, PSO has no evolution operators such as crossover and mutation. Each particle moves around the cost surface with an individual velocity. The implemented PSO algorithm updates the velocities and positions of the particles based on the local and global best solutions, according to (11) and (12), respectively.

$$v_{m,n}^{i+1} = C\left[r_0 v_{m,n}^{i} + \Gamma_1 \cdot r_1 \cdot \left(p_{m,n}^{local\,bes(i)} - p_{m,n}^{i} \right) + \Gamma_2 \cdot r_2 \cdot \left(p_{m,n}^{global\,best(i)} - p_{m,n}^{i} \right) \right] \tag{11}$$

$$p_{m,n}^{i+1} = p_{m,n}^{i} + v_{m,n}^{i+1} \tag{12}$$

Here, $v_{m,n}$ is the particle velocity; $p_{m,n}$ is the particle variables; r_0, r_1 and r_2 are independent uniform random numbers; Γ_1 is the cognitive parameter and Γ_2 is the social parameter; $p_{m,n}^{local\,best(i)}$ is the best local solution and $p_{m,n}^{global\,best(i)}$ is the best global solution; C is the constriction parameter (Kennedy & Eberhart, 1995). If the best local solution has a cost less than the cost of the current global solution, then the best local solution replaces the best global solution. PSO is a very simple bio-inspired algorithm, easy to implement and with few parameters to adjust. Flow chart shown in Fig. 4(b) gives an overview of PSO algorithm.

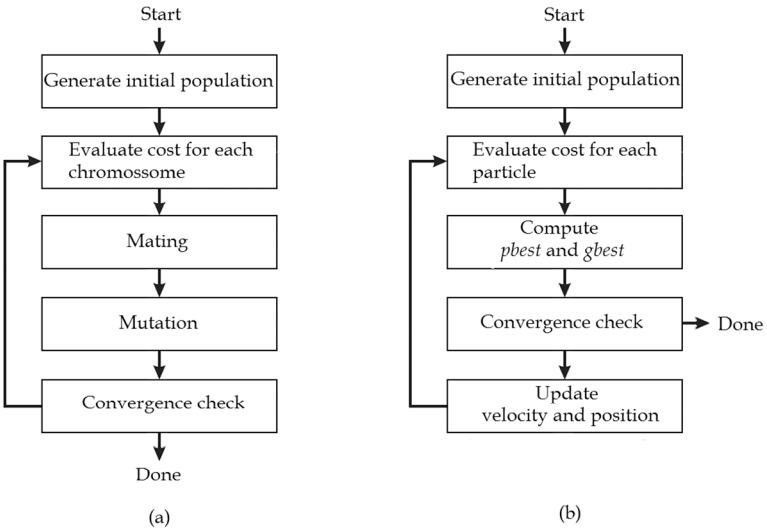

Fig. 4. Flow charts of (a) continuous-GA and (b) PSO algorithm.

3. FSS design considerations

Frequency selective surfaces (FSSs) are used in many commercial and military applications. Usually, conducting patches and isotropic dielectric layers are used to build these FSS structures. FSS frequency response is entirely determined by the geometry of the structure in one period called a unit cell. In this section is presented some considerations about the design of FSS with fractal elements for operation at the X-band (8–12 GHz) and Ku-band (12–18 GHz). FSS fabrication and measurement procedures are summarized.

3.1 Design of FSS using fractal geometries

FSS with fractal elements has attracted the attention of microwave engineering researchers because of its particular/special features. The design of a FSS with pre-fractal elements is a very competitive solution that enables the fabrication of compact spatial filters, with better performances when compared to conventional structures (Oliveira, et al., 2009; Campos et al., 2010). Several fractal iterations can be used to design a FSS with multiband frequency response associated to the self-similarity contained in the structure. Various self-similar fractals elements (e.g., Koch, Sierpinski, Minkowski, Dürer's pentagon) were previously used to design multiband FSSs (Gianvittorio et al., 2003; Cruz et al., 2009; Trindade et al., 2011).

Fig. 5 illustrates the considered periodic array in this chapter. The periodicity of the elements is given by t_x=W_c, in the x axis, and t_y=L_c, in the y axis, where W_c is the width and L_c is the length of the unit cell element; in addition, W is the width and L is the length of the patch. The design of fractal patch elements depend of desired FSS filter specifications, such as: bandstop attenuation, resonant frequency, quality factor, fabrication restrictions, etc.

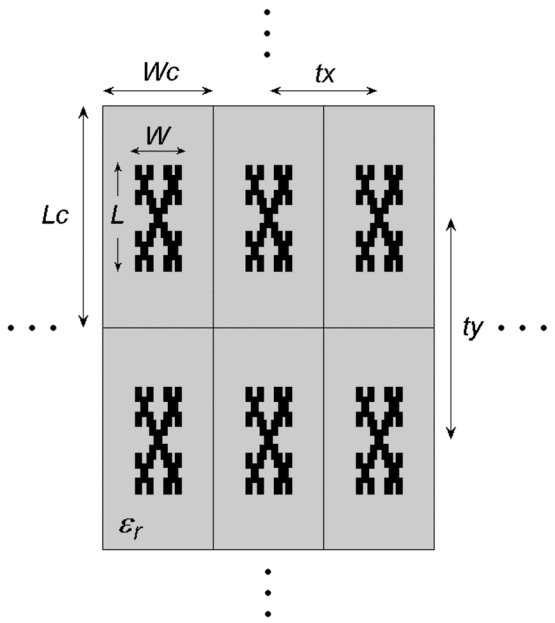

Fig. 5. Periodic array of fractal patch elements

3.1.1 Koch island fractal

The Koch island fractal patch elements were obtained assuming a rectangular construction, fractal iteration-number (or level), k=0,1,2, and a variable fractal iteration-factor $r = 1/a$, where a belongs to interval $3.05 \le a \le 10.0$. The geometry of the Koch island fractal patch elements is shown in Fig. 6, considering for k=0,1,2, and a=4. The rectangular patch element (fractal initiator) dimensions are (mm): W=4.93, L= 8.22, t_x=8.22, and t_y=12.32.

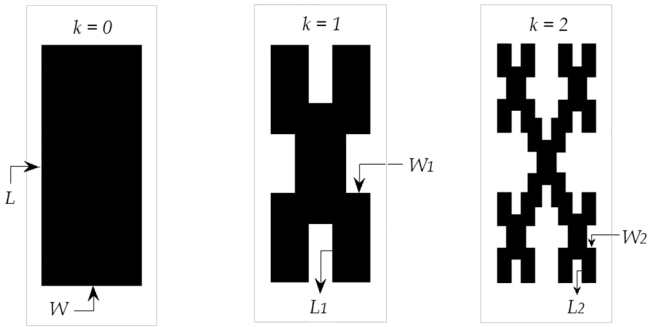

Fig. 6. Koch Island fractal patch elements (a=4)

The Koch curve begins as a straight line corresponding to each side of the conventional rectangle. Next, the Koch element in the first fractal iteration is obtained by removing four scaled rectangles (with the width and length of the initiator rectangle scaled by the fractal iteration-factor) that lies at the center of each side of the initiator rectangle. The same construction is applied for others Koch iterations (see Fig. 6). After the k-th fractal iteration, the dimensions of scaled rectangles are given in (13) through the substitution of the dummy variable ℓ_k by the width W_k or length L_k of the k-th scaled rectangle.

$$\ell_k = \begin{cases} \dfrac{\ell_{k-1}}{a}, & k = 1 \\ \dfrac{(\ell_{k-2} - \ell_{k-1})}{2a} & k = 2,3,\ldots \end{cases} \tag{13}$$

3.1.2 Dürer's pentagon fractal

The Dürer's pentagon fractal geometry was generated with the application of iterated function system (Trindade et al., 2011). From a regular pentagon patch element (L=10 mm and t_x=t_y=16.5 mm), that corresponds to the fractal initiator element, we use a fractal iteration-factor $r = 0.382$ for the generation of Dürer's pentagon elements at levels k=1,2, and 3, where $L_k = L \cdot r^k$. Therefore, six small-scale copies of the initiator element are generated in a given fractal iteration, N = 6, resulting in a fractal dimension $D = \log(N) / \log(1/r)$, where D=1.8619. The geometry of the Dürer's pentagon fractal is shown in Fig. 7.

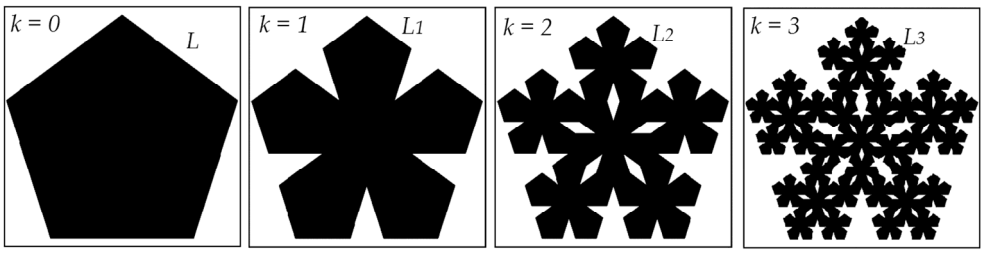

Fig. 7. Dürer's pentagon fractal patch elements

3.1.3 Sierpinski island fractal

The Sierpinski island fractal patch elements were designed based on Sierpinski curve fractal geometry. From an regular octagon patch element (L=3.6 mm and t_x=t_y=16.0 mm), that corresponds to the fractal initiator element, we used a fractal iteration-factor $r = 1/2$, and a number of five small-scale copies $N = 5$, resulting in a fractal dimension $D = \log(N)/\log(1/r)$, where D=2.3219. The geometry of the Sierpinski island fractal patch elements is shown in Fig. 8.

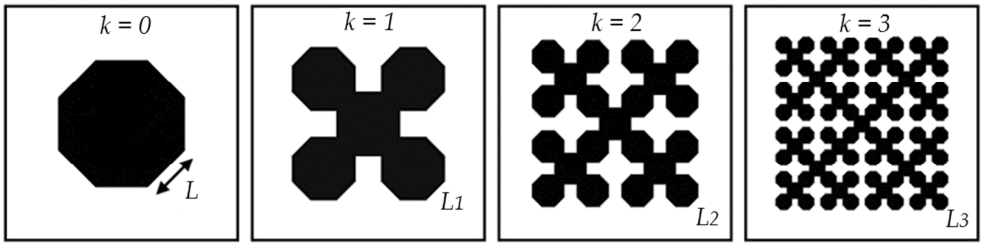

Fig. 8. Sierpinski Island fractal patch elements

3.2 Fabrication and measurement of frequency selective surfaces

The frequency selective surfaces using fractal geometries were built as periodic arrays of patch fractal elements. FSS is mounted on a dielectric isotropic layer. FSS spatial filter prototypes were fabricated using conventional planar circuit technology, with low-cost fiberglass (FR-4) substrate with 1.5 mm of height and a relative permittivity of 4.4.

The setup to measure the FSS transmission coefficients included: two horn antennas, two waveguides (cut-off frequency, 6.8 GHz), a network analyzer (model N5230A, Agilent Technologies), which operates from 300 KHz up to 13.5 GHz, beyond coaxial/waveguide transitions, handles and connectors. A fixed distance was adopted between the horn antennas in order to guarantee the operation in the far field region. The FSS filter prototypes were placed between the horn antennas for the measurement procedure (see Fig. 9).

4. Optimal design of fractal frequency selective surfaces

In this section are presented some applications of proposed optimization technique for optimal design of bandstop FSS spatial filters. Three optimization examples are described considering the use of FSS fractal patch elements: Koch island, Dürer's pentagon, and Sierpinski island. The EM characterization of these FSSs was accomplished by means of a full-wave parametric analysis through the use Ansoft Designer™ commercial software.

MLP neural network models for these FSSs were developed using the conventional EM-ANN neuromodeling technique (Zhang & Gupta, 2000). The supervised training of MLP weights was done through the well-established resilient back-propagation (RPROP) algorithm with standard training parameters (Ridmiller & Braun, 1993).

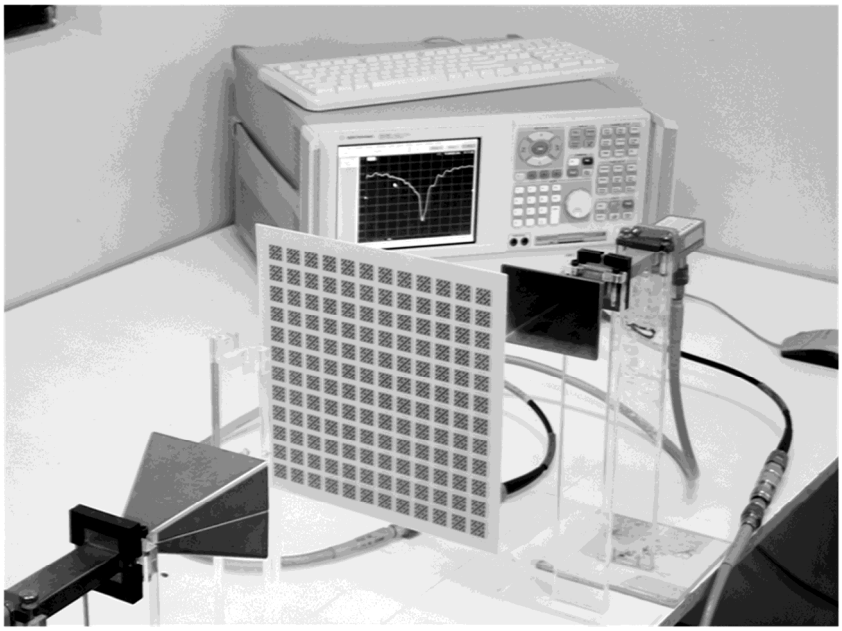

Fig. 9. Photograph of the Sierpinski FSS prototype and the measurement setup

4.1 FSS with Koch island fractal patch elements

In order to control the FSS resonant frequency and bandwidth, the shape of Koch island fractal patch elements is adjusted by fractal parameters: iteration-factor and iteration-number. The input design variables (k, a, ε_r) are limited to design region of interest defined by the following discrete values selected for MoM full-wave parametric analysis:

- Fractal iteration-number (or level): k=[1, 2]
- Fractal iteration-factor: $r = 1/a$, a=[3, 4, 5, 6, 7, 9]
- Relative permittivity: ε_r=[2.2, 3.0, 4.0, 4.8, 6.15, 7.0]
- Dielectric layer thickness: h=1.5 mm
- Scaling factors for training dataset: $\mathbf{x}_{\max} = [1, 9, 7]$ and $\mathbf{y}_{\max} = [19.05, 4.58]$

Considering for design input variables (k, a, ε_r), a MLP model was trained to approach the resonant frequency $fr(k, a, \varepsilon_r)$ and bandwidth $BW(k, a, \varepsilon_r)$ of the FSS spatial filters. The minimal MLP configuration able to solve the FSS modeling problem was defined with four input units, five hidden units, and two output units. The MLP configuration is illustrated in Fig. 10. The minimum number of five hidden neurons was found by means of a trial and error procedure and training restarts (Cruz et al., 2009).

Using sigmoid activation function, the outputs of MLP model are computed by (14).

$$\mathbf{y} = \mathbf{V} \cdot \left[-1, \frac{1}{1 + \exp(-\mathbf{W} \cdot \mathbf{x})} \right] \tag{14}$$

Where **W** and **V** are the MLP weight matrix, $\mathbf{x}=[-1, k\text{-}1, a, \varepsilon_r]^T$ and $\mathbf{y}=[fr, BW]^T$ are the MLP input and output vectors, respectively. The resultant MLP trained weight values are given by (15) and (16).

$$\mathbf{W}=\begin{bmatrix} 3.4476 & 0.4761 & 9.3218 & -0.1876 \\ 1.0630 & -0.3178 & 0.4056 & -2.0478 \\ 5.6533 & 5.2681 & 2.0179 & 1.9425 \\ 0.9611 & -4.0685 & 3.1393 & -0.1349 \\ 5.0429 & -12.4751 & 13.4767 & 1.5855 \end{bmatrix} \tag{15}$$

$$\mathbf{V}=\begin{bmatrix} -0.0572 & 0.1656 & 2.1679 & 0.1640 & 0.0936 & 0.2227 \\ 0.1059 & 0.2534 & 0.7188 & 0.2979 & 0.4961 & 0.2441 \end{bmatrix} \tag{16}$$

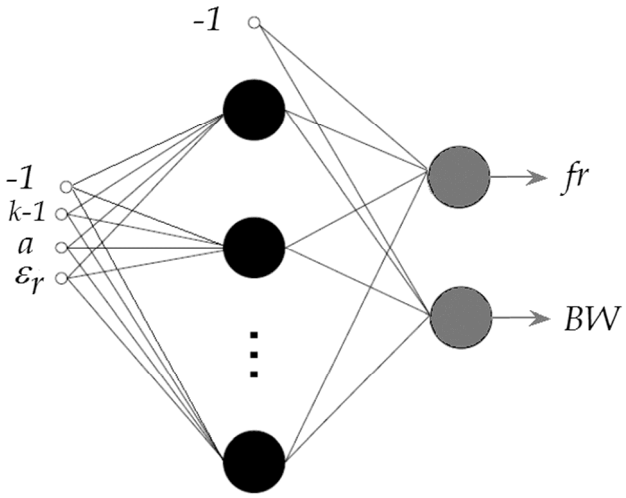

Fig. 10. Multilayer perceptron configuration

The MLP model for FSS filter design is CPU inexpensive, easy to implement and accurate. In addition, it requires small size EM dataset to learning the model of input/output mapping. The MLP model is used for evaluation of cost function in the bio-inspired optimization algorithm for FSSs with Koch island fractal patch elements.

The FSS set of design variables [*k*, *f*, *BW*] composed the input data for bio-Inspired optimization algorithms and are chosen by the user, within the region of interest of MLP model: (k=1,2), (2,7<fr<19) GHz, and (1.5<BW<4.5) GHz. Given a FSS filter desired specification (*f*, *BW*), the goal of bio-inspired optimization is to find an optimal solution (ε_r, *a*) for a given fractal level *k* that minimizes the quadratic cost function as defined in (17).

$$\mathbf{E}(i,m)=\frac{\left[f-fr\left(\mathbf{p}_m^i\right)\right]^2}{f^2}+\frac{\left[BW-BW\left(\mathbf{p}_m^i\right)\right]^2}{BW^2} \tag{17}$$

The individuals $\mathbf{p}_m^i = [\varepsilon_{rm}^i, a_m^i]^T$ evolve from the initial population given according to (18). The center of initial population $(\varepsilon_{rm}^0, a_m^0)$ in the searching space was chosen equal to (3.0, 8.5). When the population evolves, each individual is constrained to the region of interest using (19). The dummy variable ξ can be replaced by variables ε_r or a.

$$\mathbf{p}_m^0 = [randn()/5 + \varepsilon_{rm}^0 \quad randn()/5 + a_m^0] \tag{18}$$

$$\xi_m^k = \min\left(\max\left(\xi_m^k, \xi_{\min}\right), \xi_{\max}\right) \tag{19}$$

In this first FSS optimization example, we intended to verify the execution of continuous-GA and improved-GA algorithms. The algorithms start with the same initial population with 25 individuals distributed according to (18) and subject to restriction given in (19). We use the following FSS design specification: k=2, f=10.0 GHz, and BW=2.10 GHz.

Assuming the GA parameters: crossover probability=0.6, mutation rate=0.2, A=30, B=10^{-9}, $Nvar$=2, and $Npop$=25, we simulated up to 600 iterations. In Fig. 11(a) is presented the initial, intermediate, and final populations, as well as, the continuous-GA path plotted over the cost surface contours. Fig. 11(b) shows the same results for the improved-GA.

The observed zigzag paths at flat regions of the cost surface contribute to slow down the convergence of genetic algorithms. The final population of the continuous-GA algorithm oscillates around the global minimum of cost function (see Fig. 11(a)), while the improved-GA final population is closely to the global minimum (see Fig. 11(b)).

Fig. 12(a) shows the global cost evolution for the best individual of continuous-GA and improved-GA populations. It is observed that improved-GA converges closely to global minimum. The final global cost values for improved-GA and continuous-GA were 2.91×10^{-10}, and 1.26×10^{-13}, respectively. The optimized values of design parameters, $a = 5$ and $\varepsilon_r = 4.4$, were obtained (see final population in Fig. 11(b)).

To verify the optimization results, a FSS prototype with Koch island fractal patch elements was built and bandstop properties of this spatial filter were measured. In Fig. 12(b) is presented the simulated and measured FSS transmission. The obtained numeric results are presented in Table 1, and are in excellent agreement with desired FSS design specifications.

		Ansoft Designer™		Measured	
a	ε_r	f_r (GHz)	BW (GHz)	f_r (GHz)	BW (GHz)
5	4.4	9.97	2.10	10.00	1.73

Table 1. Simulated and measured results of optimized FSS

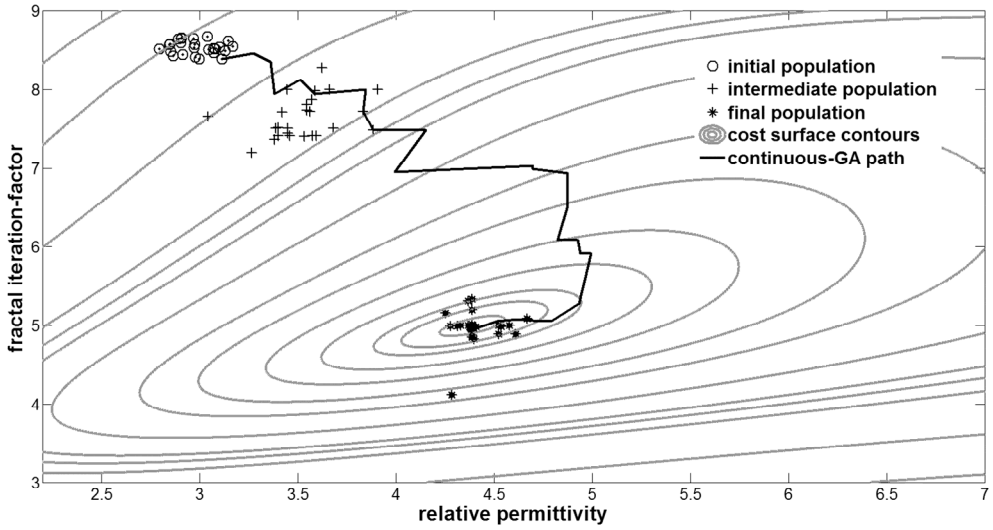

(a)

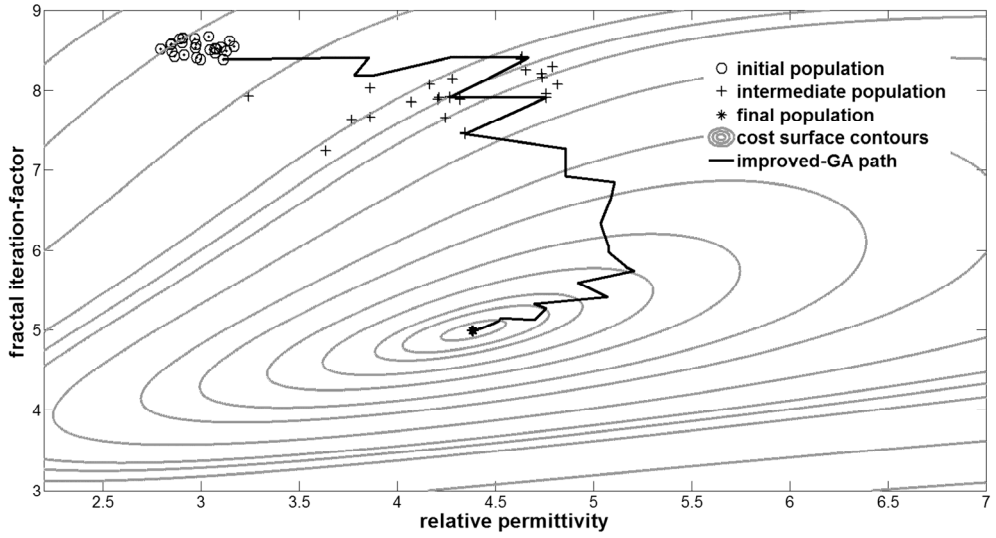

(b)

Fig. 11. Initial, intermediate, and final populations and GA paths plotted over the cost surface contours: (a) continuous-GA and (b) improved-GA.

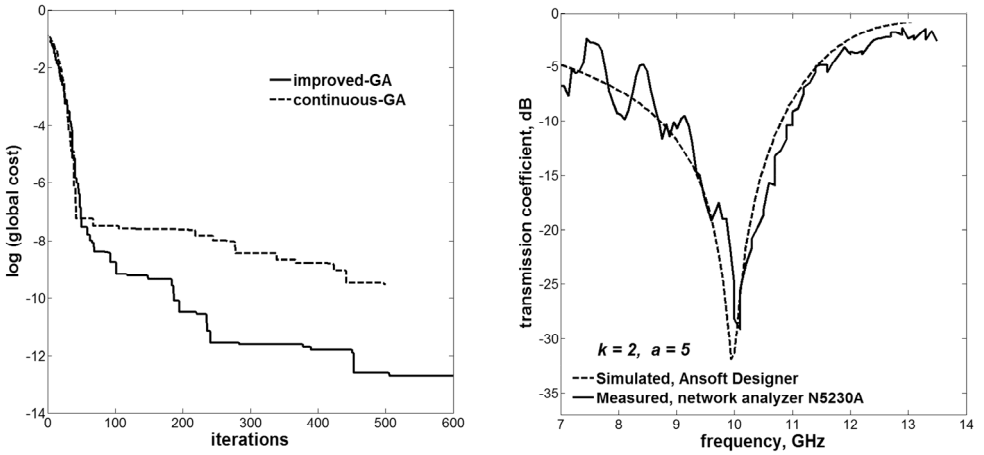

(a) (b)

Fig. 12. (a) Evolution of global cost for continuous-GA and improved-GA. (b) Comparison between the simulated and measured FSS transmission (k=2, ε_r=4.4, and a =5)

4.2 FSS with Dürer's pentagon patch elements

The Dürer's pentagon geometry was used to design a FSS consisting of a periodic array of fractal patch elements. The input design variables (k, $\tan\delta$, t_x, ε_r) are limited to design region of interest defined by the following discrete values selected for parametric analysis:

- Fractal iteration-number (or level): k=[0, 1, 2, 3]
- Patch element periodicity: t_x=t_y= [16.5, 17, 18, 19, 20, 21, 22, 23, 24, 25] mm
- Relative permittivity: ε_r=[2.33, 3.5, 4.4, 6.15, 10.2]
- Loss tangent: $\tan\delta$ = [0.0014, 0.012, 0.02, 0.0025, 0.0035]
- Dielectric layer thickness: h=1.5 mm

Considering for design input variables (k, $\tan\delta$, t_x, ε_r), a MLP model was trained to approach the resonant frequency and bandwidth of the bandstop FSS spatial filters. The minimal MLP configuration able to solve the FSS modeling problem was defined with five input units, ten hidden units, and two output units.

The MLP model outputs are shown in Fig. 13(a) and 13(b), considering the limits of the desired region of interest of the design input variables. The MLP model is able to interpolate the training examples corresponding to ε_r=[2.33, 3.5, 6.15, 10.2] and presents generalization ability for new inputs within the region of interest, ε_r=4.4. Thus, the MLP model learns the EM behavior of FSS filters becoming available this EM knowledge for future utilization.

In this second FSS optimization example, we verify the performance of continuous-GA and PSO. The algorithms start with the same initial population with $Npop$=25 individuals $\mathbf{p}_m^i = [\varepsilon_{rm}^i, t_{xm}^i]^T$ distributed according to (18) with $(\varepsilon_{rm}^0, t_{xm}^0)$ = (9.0, 24).

The FSS set of design variables [k, f, BW] composed the input data for bio-Inspired optimization algorithms and are chosen by the user, within the region of interest of MLP

model: (k=0,1,2,3), (4.9<fr<13.9) GHz, and (0.6<BW<4.6) GHz. In this example, we use the following FSS design specification: k=1, f=8.2 GHz and BW=2.78 GHz.

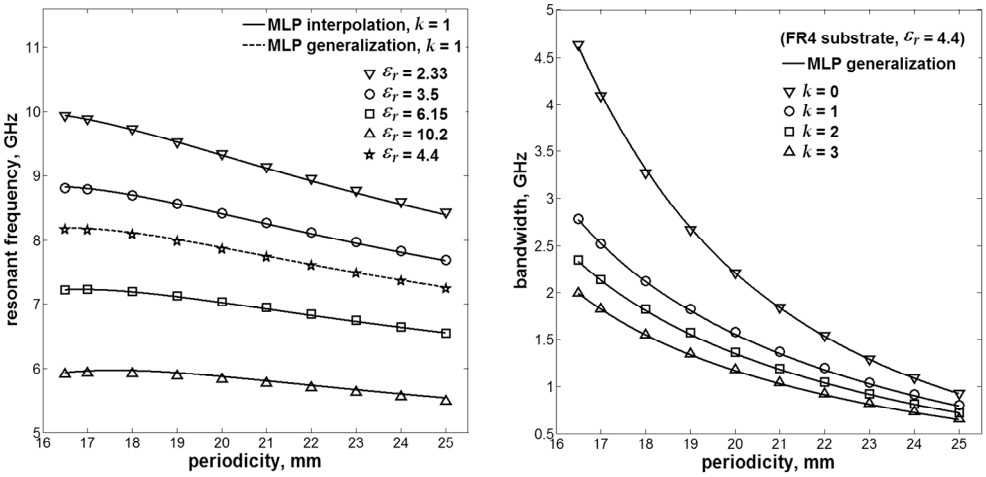

(a) (b)

Fig. 13. (a) FSS resonant frequency as a function of periodicity and relative permittivity. (b) FSS bandwidth as a function of periodicity and fractal iteration-number

Assuming the genetic algorithm parameters: crossover probability=0.6, mutation rate=0.2, A=30, B=10^{-9}, $Nvar$=2 and $Npop$=25, we simulated up to 250 GA-iterations. Fig. 14(a) shows the initial, intermediate and final populations, and the continuous-GA path plotted over the cost surface contours. The optimal solution was: ε_r=4.4 and t_x=t_y=16.5 mm.

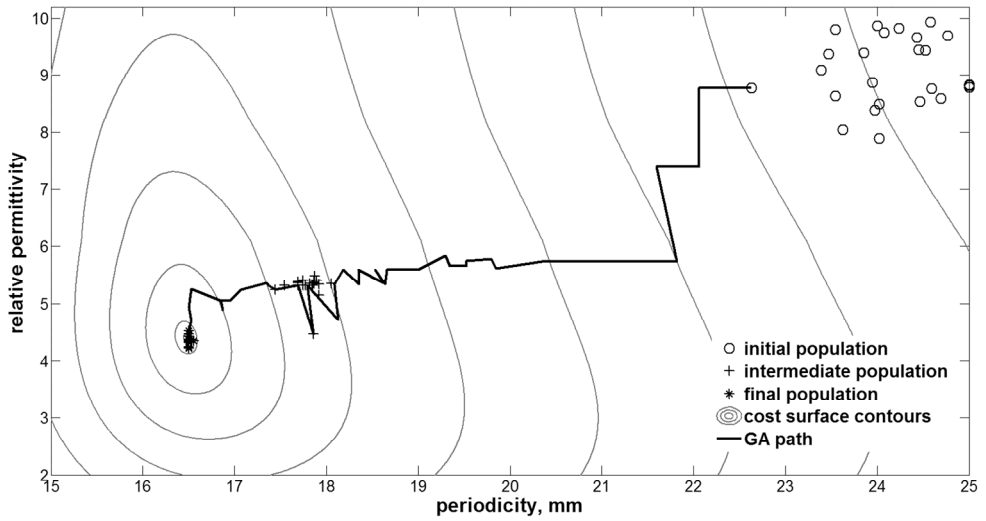

(a)

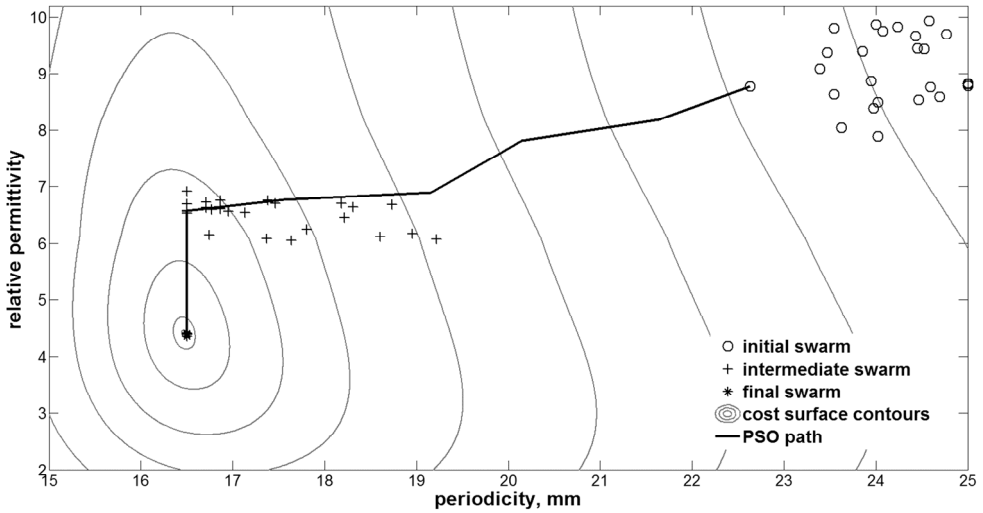

(b)

Fig. 14. Initial, intermediate, and final populations and bio-inspired algorithm paths plotted over the cost surface contours: (a) continuous-GA and (b) PSO.

The PSO algorithm with parameters $\Gamma_1 = \Gamma_2 = 2$, $C = 1.3$ and the same initial population was used for FSS optimization. Fig. 14(b) shows the PSO path plotted over the cost surface contours. In this simulation, the PSO algorithm converges to the global minimum of cost function after 96 iterations. In this case, the optimal solution was: ε_r=4.4 and t_x=t_y=16.5 mm.

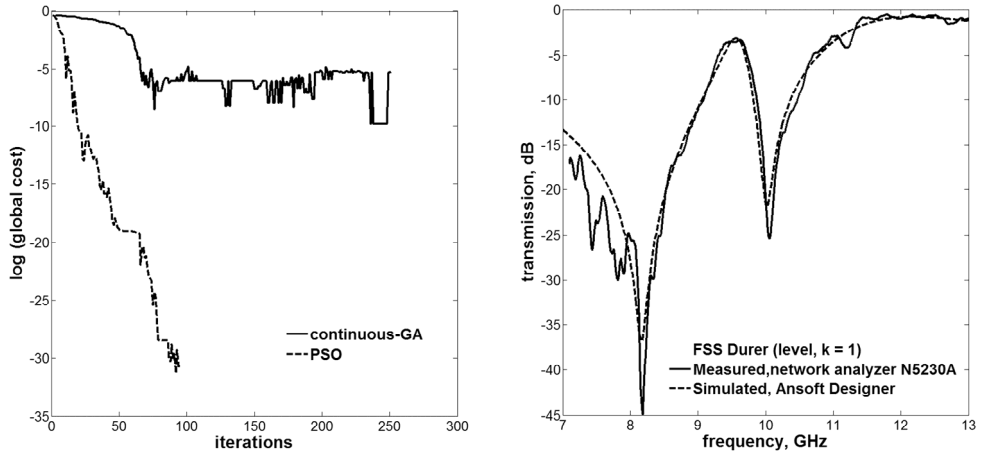

Fig. 15. (a) Evolution of global cost for continuous-GA and PSO. (b) Comparison between the simulated and measured FSS transmission (k=1, ε_r=4.4, and t_x=t_y=16.5 mm).

Fig. 15(a) shows the evolution of the average global cost for continuous-GA and PSO populations. We observe that the PSO algorithm is limited in precision to the round off error

of the computer (≈10^{-31}). In Fig. 15(b) is presented a comparison between the simulated and measured results for the transmission coefficient (dB) of the optimized FSS with Koch fractal patch elements. The simulated and measured results are in excellent agreement with desired FSS design specifications.

4.3 FSS with Sierpinski ilsland fractal patch elements

The Sierpinski island fractal geometry was used to design a FSS consisting of a periodic array of fractal patch elements. The input design variables (k, t_x, ε_r) are limited to design region of interest defined by the following discrete values selected for parametric analysis:

- Fractal iteration-number (or level): k=[1, 2, 3]
- Patch element periodicity: t_x=t_y=[15, 16, 17, 18, 19, 20, 21, 22, 23, 24, 25] mm
- Relative permittivity: ε_r=[2.2, 2.94, 4.4, 6.15, 10.2]
- Dielectric layer thickness: h=1.5 mm

Considering for design input variables (k, ε_r, t_x), a MLP model was trained to approach the resonant frequency and bandwidth of the FSS filters with Sierpinski island fractal patch elements. Fig. 16 shows the variation of sum squared error given in (6) as a function of the number of MLP hidden units. The minimal MLP configuration able to solve the FSS modeling problem was defined with four input units, fifteen hidden units, and two output units.

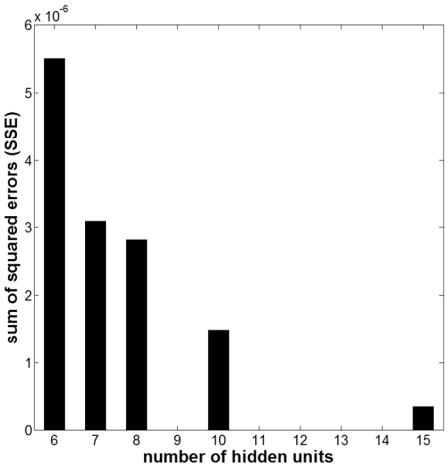

Fig. 16. Variation of SSE as a function of MLP hidden units

The MLP model outputs are shown in Fig. 17(a) and 17(b). Considering the limits of the desired region of interest of the input design variables, the MLP model is able to interpolate the training dataset.

In this third FSS optimization example, we intended to verify the execution of continuous-GA, improved-GA, and PSO. The algorithms start with the same initial population with $Npop$=100 individuals $\mathbf{p}_m^i = [\varepsilon_{rm}^i, t_{xm}^i]^T$ distributed according to (18), with $(\varepsilon_{rm}^0, t_{xm}^0)$ = (8.5, 22) and subject to restriction given in (19).

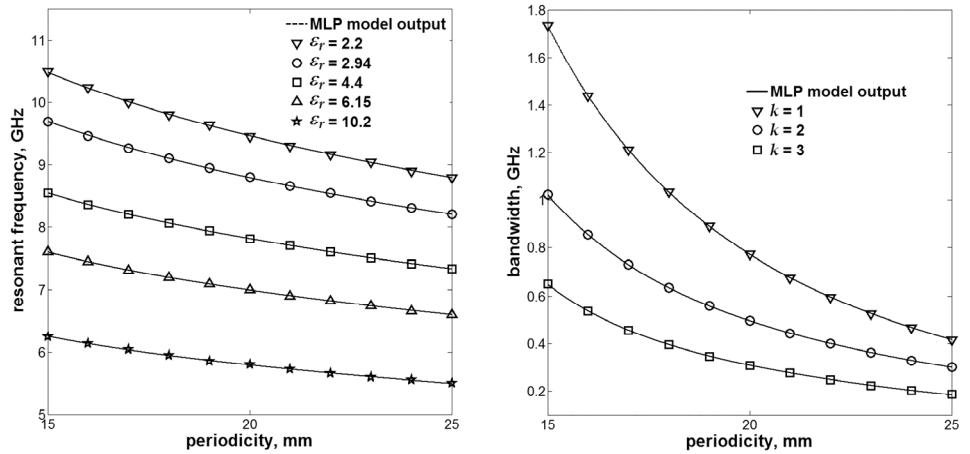

Fig. 17. (a) FSS resonant frequency as a function of periodicity and relative permittivity. (b) FSS bandwidth as a function of periodicity and fractal levels

The FSS design variables [*k*, *f*, *BW*] composed the input data for bio-Inspired optimization algorithms and are chosen by the user within the region of interest of MLP model: (*k*=1,2,3), (3.1<*fr*<10.5) GHz, and (0.15<*BW*<1.7) GHz. We used the following input data for simulation of bio-inspired optimization: *k*=1, *f*=8.37 GHz and *BW*=1.44 GHz.

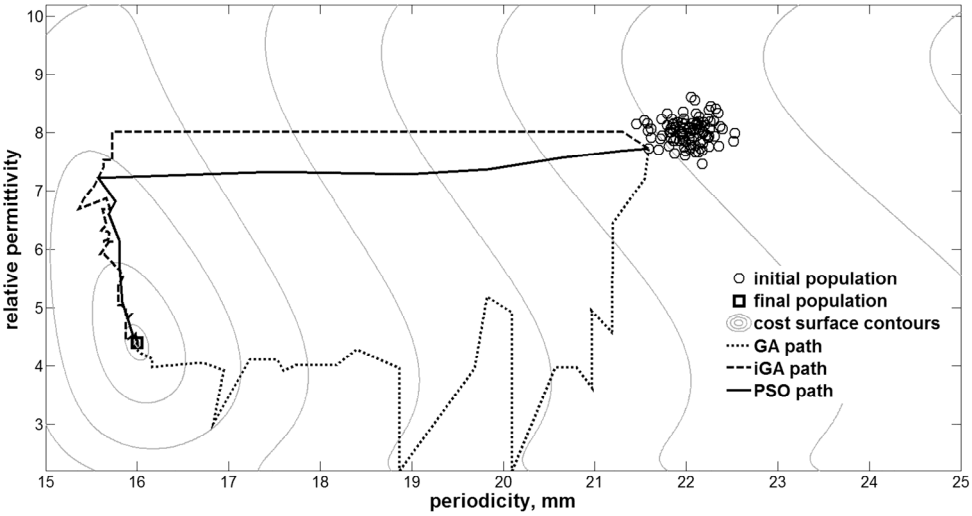

Fig. 18. Bio-inspired algorithm paths plotted over the cost surface contours, initial, intermediate, and final populations

In Fig. 18 is presented the initial, intermediate, and final populations, as well as, the bio-inspired algorithm paths plotted over the cost surface contours. In this case, the optimal solution founded was: ε_r=4.4 and t_x=t_y=16.0 mm.

Fig. 19(a) shows the evolution of the global cost for bio-inspired algorithms. PSO algorithm converges to the global minimum of cost function after 93 iterations. Improved-GA and continuous-GA converge after 185 and 211 iterations, respectively. In this example, implemented bio-inspired algorithms are limited in precision to the round off error of the computer ($\approx 10^{-31}$). In Fig. 19(b) is presented a comparison between the CPU requirement as a function of bio-inspired algorithm iterations. From this result, was observed that the CPU spent-time of bio-inspired optimization is determined by MLP model CPU requirement.

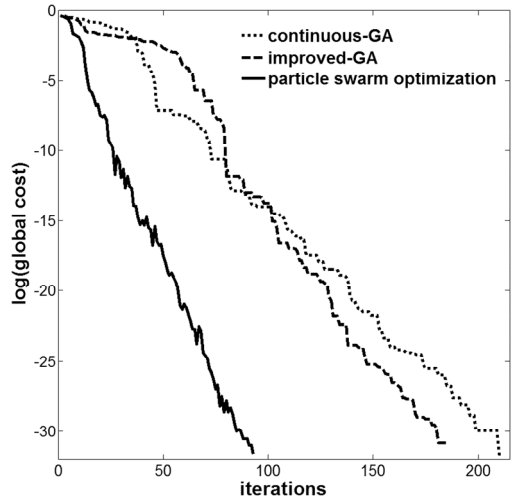

(a)

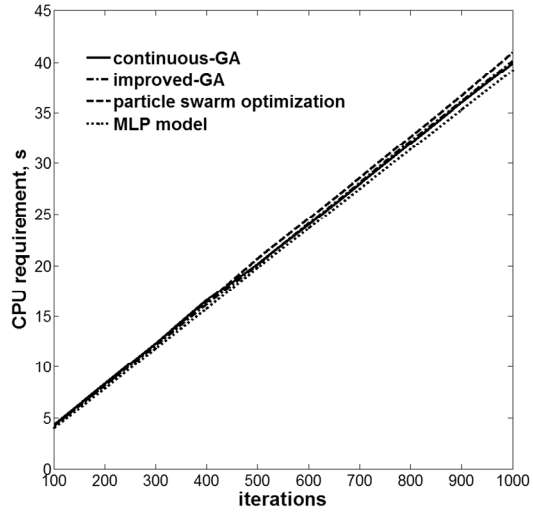

(b)

Fig. 19. (a) Evolution of global cost for implemented bio-inspired algorithms. (b) CPU requirement as a function of bio-inspired algorithm iterations (*Npop*=100)

Fig. 20(a) shows a photograph of the fabricated FSS prototype with Sierpinski island fractal patch elements considering the optimal design parameters: k=1, ε_r=4.4, and t_x=t_y=16.0 mm. In Fig. 20(b) is presented a comparison between the simulated and measured results for the transmission coefficient (dB) of the optimized FSS. The simulated and measured results are in good agreement with desired FSS design specifications (f=8.37 GHz and BW=1.44 GHz).

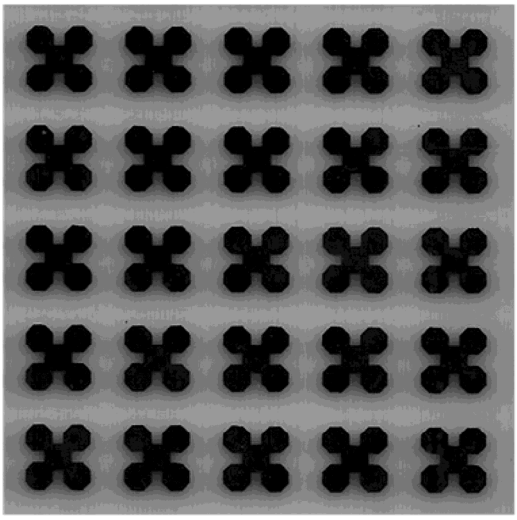

(a)

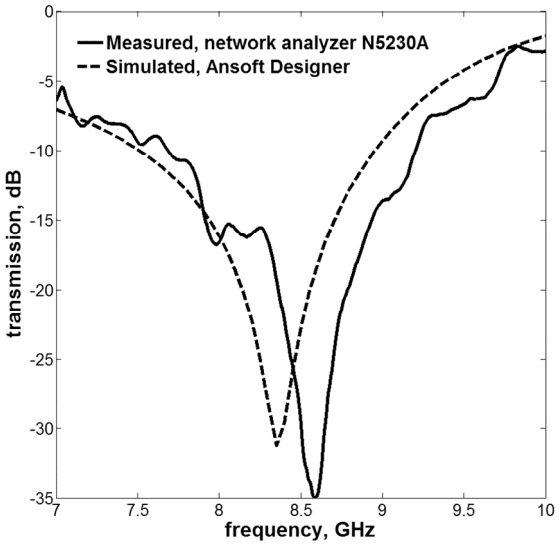

(b)

Fig. 20. (a) Built FSS prototype with Sierpinski island fractal patch elements (k=1, ε_r=4.4, and t_x=t_y=16.0 mm). (b) Comparison between the simulated and measured FSS transmission

5. Conclusion

This chapter described a new EM optimization technique blending full-wave method of moments, MLP artificial neural networks and bio-inspired algorithms for optimal design of frequency selective surfaces with fractal patch elements. Three fractal geometries were considered: Koch island, Dürer's pentagon and Sierpinski island. The use of fractal geometries to design FSS on isotropic dielectric substrates becomes possible the control of its frequency responses without increase its overall size. The MLP models were trained with accurate EM data provided by FSS simulations based on the method of moments. The computation of cost function of bio-inspired algorithms was done throught the use of developed MLP models. This procedure results in fast and accurate bio-inspired optimization algorithms. According to the obtained results, genetic algorithms present zigzag paths at flat regions of the cost surface that contribute to slow down the algorithm convergence. The introdution of a new mutation operation avoid the oscilation of continuous-GA final population around the global minimum of cost function. The improved-GA final population closely to the global minimum improves the GA convergence. PSO algorithm showed to be faster and easier to implement. This makes the optimization through PSO a powerful tool in synthesizing FSS structures. The idea of blending bio-inspired algorithms and artificial neural networks to optimize frequency selective surfaces shows to be very interesting, due to its great flexibility and easy application to structures that do not have a direct fitness function. The MoM-ANN-GA/PSO proposed technique is accurate and CPU inexpensive, which are most desired characteristics in the development of computer-aided design tools for EM optimization.

6. Acknowledgment

This work was supported by CNPq, under contracts 479253/2009-9 and 307256/2009-0, by Federal Institute of Education, Science and Technology of Paraíba (IFPB) and by Federal University of Rio Grande do Norte (UFRN).

7. References

Bandler, J. W. et al. (1994). Space Mapping Technique for Electromagnetic Optimization. *IEEE Transactions on Microwave Theory and Techniques*, Vol.42, No.12, (December 1994), pp. 2536-2544, ISSN 0018-9480

Bandler, J. W. et al. (1996). Parameterization of Arbitrary Geometrical Structures for Automated Electromagnetic Optimization, *Proceedings of IEEE MTT-S International Microwave Symposium Digest*, pp. 1059-1062, ISBN 0-7803-3246-6, San Francisco, CA, USA, August 17-21, 1996

Campos, A. L. P. S., Oliveira, E. E. C. & Silva, P. H. F. (2010). Design of Miniaturized Frequency Selective Surfaces Using Minkowski Island Fractal, *Journal of Microwaves, Optoelectronics and Electromagnetic Applications*, Vol.9, No.1, (June 2010), pp. 43-49, ISSN 1516-7399

Cruz, R. M. S.; Silva, P. H. F. & D'Assunção, A. G. (2009). Neuromodeling Stop Band Properties of Koch Island Patch Elements for FSS Filter Design, *Microwave and Optical Technology Letters*, Vol.51, No.12, (December 2009), pp. 3014-3019, ISSN 1098-2760

Fahmi, M. (November 2007). Computer Aided Design of Wide-Band Microwave
Components, In: *Digital Repository at the University of Maryland,* 18.10.2011, Available from http://drum.lib.umd.edu/handle/1903/7693

Gianvittorio, J. P. et al., (2001). Fractal FSS: Various Self-Similar Geometries Used for Dual-Band and Dual-Polarized FSS. *Proceedings of the IEEE Antennas and Propagation Society International Symposium*, pp. 640-643, ISBN 0-7803-7070-8, Boston, MA , USA, July 8-13, 2001

Gianvittorio, J. P. et al., (2003). Self-Similar Prefractal Frequency Selective Surfaces for Multiband and Dual-Polarized Applications, *IEEE Transactions on Antennas and Propagation*, Vol.51, No. 11, (November 2003), pp. 3088-3096, ISSN 0018-926X

Haupt, R. L. (1995). An introduction to Genetic Algorithms for Electromagnetics. *IEEE Antennas Propagation Magazine*, Vol.37, No.2, (April 1995), pp. 7-15, ISSN: 1045-9243

Haupt, R. L. & Haupt, S. E. (2004). *Practical Genetic Algorithms*, 2nd ed., Wiley, ISBN 978-0-471-45565-3, New Jersey, NJ, USA

Haupt, R. L. & Werner, D. H. (2007). *Genetic algorithms in electromagnetics*. Willey, ISBN 978-0-471-48889-7, Hoboken, NJ, USA

Haykin, S. (1999). *Neural Networks: A Comprehensive Foundation*, (2nd ed.), Prentice-Hall, ISBN 0-13-273350-1, Upper Saddle River, NJ, USA

Hussein, Y. A. & El-Ghazaly, S. M. (2004). Modeling and Optimization of Microwave Devices and Circuits Using Genetic Algorithms, *IEEE Transactions on Microwave Theory and Techniques*, Vol.52, No.1, (January 2004), pp. 420-435, ISSN 0018-9480

Kennedy, L. & Eberhart, R. C. (1995). Particle swarm optimization. *Proceedings of the IEEE International Conference on Neural Networks*, pp. 1942-1948, ISBN 0-7803-2768-3, Perth, WA , Australia, November 27-01, 1995

Manara, G. et al., (1999). Frequency Selective Surface Design Based on Genetic Algorithm, *Electronics Letters*, Vol.35, No.17, (August 1999), pp. 400-401, ISSN 0013-5194

Mohamed, A. S. (August 2005). Recent Trends in CAD Tools for Microwave Circuit Design
Exploiting Space Mapping Technology, In: *CiteSeer,* 18.10.2011, Available from http://sos.mcmaster.ca/theses/ahmed%20mohamed/

Munk, B. A. (2000). *Frequency-Selective Surfaces: Theory and Design*. Wiley, ISBN 0-471-37047-9 New York, NY, USA

Nikolova, N. K. et al. (2004). Adjoint Techniques for Sensitivity Analysis in High-Frequency Structure CAD, *IEEE Transactions on Microwave Theory and Techniques*, Vol.52, No.1, (January 2004), pp. 403-419, ISSN 0018-9480

Patnaik, A. & Mishra, R. K. (2000). ANN Techniques in Microwave Engineering. *IEEE Microwave Magazine,* Vol.1, No.1, (March 2000), pp. 55-60, ISSN 1527-3342

Ridmiller M. & Braun, H. (1993). A Direct Adaptative Method for Faster Backpropagation Learning: the RPROP Algorithm. *Proceedings of the IEEE International Conference on Neural Networks*, pp. 586-591, ISBN 0-7803-0999-5, San Francisco, CA , USA, March 28-01, 1993

Santos, A. L., Romariz, A. R. S. & Carvalho, P. H. P. (1997). Neural model of electrical devices for circuit simulation. *Proceedings of the SBMO/IEEE MTT-S International Microwave and Optoelectronics Conference*, Vol. 1, No.1, pp. 253-258, ISBN 0-7803-4165-1, Natal, Brazil, August 11-14, 1997

Silva, P. H. F., Lacouth, P., Fontgalland, G., Campos, A.L.P.S. & D'Assuncao, A.G. (2007). Design of Frequency Selective Surfaces Using a Novel MoM-ANN-GA Technique.

Proceedings of the SBMO/IEEE MTT-S International Microwave and Optoelectronics Conference, Vol.1, No.1, pp. 275-279, ISBN 978-1-4244-0661-6, Salvador, Brazil, October 29-1, 2007

Silva, P. H. F. et al. (2010a). Neuromodeling and Natural Optimization of Nonlinear Devices and Circuits, In: *System and Circuit Design for Biologically Inspired Intelligent Learning,* Turgay Temel, pp. 326-348, IGI Global, ISBN 978-1-60960-020-4, New York, NY, USA

Silva, P. H. F. et al. (2010b). Blending PSO and ANN for Optimal Design of FSS Filters With Koch Island Patch Elements. *IEEE Transactions on Magnetics*, Vol.46, No.8, (August 2010), pp. 3010-3013, ISSN 0018-9464

Trindade, J. I. A. et al. (2011). Analysis of Stop-Band Frequency Selective Surfaces With Dürer's Pentagon Pre-Fractals Patch Elements. *IEEE Transactions on Magnetics*, Vol.47, No. 5, (May 2011), pp. 1518-1521, ISSN 0018-9464

Oliveira, E. E. C.; Campos, A. L. P. S. & Silva, P. H. F. (2009). Miniaturization of Frequency Selective Surfaces Using Fractal Koch Curves. *Microwave and Optical Technology Letters*, Vol.51, No.8, (August 2009), pp. 1983-1986, ISSN 1098-2760

Zhang, Q. J. & Gupta, C. (2000). *Neural Networks for RF and Microwaves Design,* Artech House, ISBN 1-781-769-9750, Norwood, MA, USA

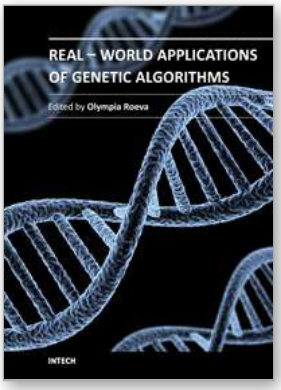

Real-World Applications of Genetic Algorithms
Edited by Dr. Olympia Roeva

ISBN 978-953-51-0146-8
Hard cover, 376 pages
Publisher InTech
Published online 07, March, 2012
Published in print edition March, 2012

The book addresses some of the most recent issues, with the theoretical and methodological aspects, of evolutionary multi-objective optimization problems and the various design challenges using different hybrid intelligent approaches. Multi-objective optimization has been available for about two decades, and its application in real-world problems is continuously increasing. Furthermore, many applications function more effectively using a hybrid systems approach. The book presents hybrid techniques based on Artificial Neural Network, Fuzzy Sets, Automata Theory, other metaheuristic or classical algorithms, etc. The book examines various examples of algorithms in different real-world application domains as graph growing problem, speech synthesis, traveling salesman problem, scheduling problems, antenna design, genes design, modeling of chemical and biochemical processes etc.

How to reference
In order to correctly reference this scholarly work, feel free to copy and paste the following:

Paulo Henrique da Fonseca Silva, Marcelo Ribeiro da Silva, Clarissa de Lucena Nóbrega and Adaildo Gomes D'Assunção (2012). Application of Bio-Inspired Algorithms and Neural Networks for Optimal Design of Fractal Frequency Selective Surfaces, Real-World Applications of Genetic Algorithms, Dr. Olympia Roeva (Ed.), ISBN: 978-953-51-0146-8, InTech, Available from: http://www.intechopen.com/books/real-world-applications-of-genetic-algorithms/application-of-bio-inspired-algorithms-and-neural-networks-for-optimal-design-of-fractal-frequency-s

INTECH
open science | open minds

InTech Europe
University Campus STeP Ri
Slavka Krautzeka 83/A
51000 Rijeka, Croatia
Phone: +385 (51) 770 447
Fax: +385 (51) 686 166
www.intechopen.com

InTech China
Unit 405, Office Block, Hotel Equatorial Shanghai
No.65, Yan An Road (West), Shanghai, 200040, China
中国上海市延安西路65号上海国际贵都大饭店办公楼405单元
Phone: +86-21-62489820
Fax: +86-21-62489821

© 2012 The Author(s). Licensee IntechOpen. This is an open access article distributed under the terms of the Creative Commons Attribution 3.0 License, which permits unrestricted use, distribution, and reproduction in any medium, provided the original work is properly cited.